

An Adaptive Computational Model for Predicting the Density Distribution of the Proximal Femur

A. Brereton¹, G. Warner¹, L. Burge²

A. Marzban³, H. Nayeb-Hashemi³,

1. Dept. of Mechanical Engineering,

2. Dept. of System and Computer Science, Howard University, Washington DC 20059

3. Dept. of Mech. and Industrial Eng., Northeastern University, Boston, MA 02115

ABSTRACT

A custom algorithm was developed to simulate adaptive bone remodeling. The process of adaptive bone remodeling can be simulated with a self-optimizing finite element method (FEM). The basic remodeling rule attempts to obtain a constant value for the strain energy per unit bone mass, by adapting density. The precise solution is dependent on the loads, initial conditions and the parameters in the remodeling rule. The aim of this study was to identify how the bone density distribution of the proximal femur was affected by parameters which govern the remodeling process. The forces at different phases of the gait cycle were applied as boundary conditions. The bone density distributions from these forces were averaged to estimate the density distribution in the proximal femur. The effect of varying the spatial influence function, and the influence range on the converged solution were investigated. It was shown that varying these parameters within reasonable upper and lower bounds had very little impact on the qualitative form of the converged solution. In all cases, the solutions obtained are comparable with the actual density in the proximal femur, as measured by DEXA scans.

KEYWORDS

Bone Remodeling, Finite Element Method, Computational Engineering

INTRODUCTION

Research regarding bone structures can be traced back to Galileo (1638), who is credited with applying his understanding of beam bending to the mechanical analysis of bone. Wolff (1892), observed that bone is reshaped in response to the forces acting on it (Wolff's law). Several investigations have been made to augment and verify 'Wolff's Law' by rigorous mathematical procedures. Roux (1881) suggested that bone cells could sense and respond to mechanical stress. Wolff's law is still the basis of modern theories relating bone cellular adaptation to stress.

One of the fundamental theories of bone remodeling is the theory of adaptive elasticity as suggested by Cowin et al. (1976), Hegedus et al. (1976) and Firoozbakhsh et al. (1981). This theory is based on general continuum mechanics principles. The computational implementation of this theory using finite element modeling was conducted by Hart et al. (1984). Huiskes et al. (1987, 1992), Kerner et al. (1999) and Turner et al. (2005) utilized a homeostatic zone in their

adaptive bone density studies. The essential idea was that above a certain level of strain or strain energy, bone density was increased and below a certain criteria, bone density was decreased. The bone structure remains unchanged, between these two levels. Weinans et al. (1992), Xinghua et al. (2002, 2005) considered the strain energy density (SED) as the stimulus and defined the bone density adaptation algorithm as,

$$\frac{d\rho}{dt} = B \left(\frac{U_a}{\rho} - k \right) \quad 0 < \rho \leq \rho_{cb} \quad (1)$$

where $U_a = \frac{1}{n} \sum_{i=1}^n U_i$; and U_i is apparent strain energy density (SED) for loading case i and n is the total number of loading cases, B and reference value k are constants. ρ_{cb} is the maximal density of bone which usually considered as the density of cortical bone.

Mullender et al (1994), proposed that the osteocytes act as sensors. Each sensor produces a stimulus for mass regulation in its vicinity, and its effect attenuates exponentially from the sensor's location. The concept of a spatial influence function $f_i(r)$ was introduced, which was used to describe the attenuation of stimulus between osteocyte i and location r . Each actor cell received stimulus from all sensor cells. The contribution of each sensor to the actor cell depends on their location respect to the actor cell.

The purpose of this study is to obtain a better understanding of the influence of important parameters on the behavior of the strain energy-adaptive bone-remodeling simulation. In particular, the density distribution, stability and convergence of the remodeling rule are investigated by changing the initial conditions, spatial influence function $f_i(r)$, and its parameters.

ADAPTIVE MODELING METHOD

In our present paper, we have studied the effects of different parameters in the remodeling rule. The bone density remodeling is adopted from Huiskes et al. (1987, 1992) and Xinghua et al. (2002, 2005), and is presented as,

$$\frac{d\rho(r,t)}{dt} = B(t) \left(\sum_{i=1}^N f_i(r) (\beta_i^\alpha - 1) \right) \quad 0 < \rho \leq \rho_{cb} \quad (2)$$

where $\beta_i = \frac{U_a(i)}{\rho_i k}$

where N is the number of sensor cells and $f_i(r)$ is a spatial influence function which brings the effect of density change from a sensor location to adjacent cells, i.e. $f_i(r) = e^{-r/R}$; r_i is the distance between osteocyte i and location r and R is the influence distance. Here we have taken a range for R values in order to understand its effect on the converged bone density and the convergence rate. β is called a comparative coefficient, describing the comparison of mechanical stimulus $U_a(i)/\rho_i$ in each sensor cell with reference value k . $U_a(i)/\rho_i$ is measured per element, assuming one sensor per element, and the apparent density is also adapted per element. $B(t)$ is the remodeling coefficient, which decreases gradually with the iteration time. α is the order of non-linear remodeling equation and it is a constant during the iteration process. For the finite element procedure, the ANSYS finite element code was used (ANSYS, Inc., Southpointe, 275 Technology Drive, Canonsburg, PA, 15317).

The coefficient $B(t)$ and other parameters for the initial investigation were adopted from the work by Xinghua et al. (2002, 2005),

$$\left. \begin{aligned} B(t) &= (B_0 - B_r) / e^{0.02t} + B_r \\ \text{where } B_0 &= 0.165 \text{ gr/cm}^3 \cdot \text{sec} \\ B_r &= 0.05 \text{ gr/cm}^3 \cdot \text{sec} \\ k &= 0.1125 \text{ J/gr} \\ \text{initial } \alpha &= 1.5 \\ \rho_{\min} &= 0.01 \text{ gr/cm}^3 \\ \rho_{\max} &= 1.74 \text{ gr/cm}^3 \\ f_i(r) &= e^{-r/R} \\ \text{initial } R &= 0.1 \text{ cm} \end{aligned} \right\} (3)$$

The minimal density was assumed to be 0.01 gr/cm^3 , representing complete resorption of an element. The maximal density was taken as 1.74 gr/cm^3 which is the apparent density of cortical bone. The density of trabecular, or cancellous, bone varies between $0.01 - 1.74 \text{ gr/cm}^3$.

The value of “R” in spatial function has a significant effect on the convergence. The convergence was not achieved with improper R selection which will be discussed later in more detail. The effect of R on $f_i(r)$ function is shown in Fig. 1. Each element has three possibilities to converge and reach remodeling equilibrium: (1) the bone is completely resorbed ($\rho = \rho_{\min} = 0.01 \text{ gr/cm}^3$); (2) the bone becomes cortical ($\rho = \rho_{\max} = 1.74 \text{ gr/cm}^3$); or (3) the bone remains cancellous with an apparent density satisfying Eq. (2). Hence, the remodeling equilibrium condition determined from bone remodeling theory is

$$\rho = \rho_{\min} \quad \text{or} \quad \rho = \rho_{\max} \quad \text{or} \quad \frac{d\rho}{dt} = 0, \quad \text{i.e.} \quad \frac{U}{\rho} = k \quad (4)$$

A two-dimensional finite element model of a proximal femur was constructed as shown in Fig. 2. The model was meshed by 2628 four nodes elements. In this study, we considered loading during the loading response, mid-stance, and push off phases of the gait cycle (stance phase). These were also considered by Huiskes et al. (1987, 1992) and Xinghua et al. (2002, 2005). However, this study is novel, in that we allow the solution from each loading phase to converge and then average the solutions to obtain the final bone density distribution. The adaptive bone remodeling algorithm is implemented via the APDL programming language and takes input from FEA software. Huiskes et al. (1987, 1992) and Xinghua et al. (2002, 2005) averaged the strain energy density from all phases of the gait cycle and then applied the adaptive algorithm. Our results show that this scheme is more effective than those proposed by Huiskes et al. (1987, 1992) and Xinghua et al. (2002, 2005), in smoothing sharp density gradients present in prior work. A typical loading condition to the proximal femur corresponding to the heel strike is shown in Fig. 2. This loading was used in the finite element analyses and adaptive bone density algorithms. Table 1 shows the magnitude of loads at various points in the gait cycle.

Table 1. Applied Loads to the proximal femur at different phases of the gait cycle based on Bitsakos et al. (2005)

Joint Contact & Muscle Forces	Muscle force components (N)					
	10% gait cycle (loading response)		30% gait cycle (mid stance)		45% gait cycle (push off)	
	X	Y	X	Y	X	Y
Hip Joint contact force	-	-	-	-	-	-
	857.3	1722.5	861.3	2056.9	613.7	2868.7
Piriformis	75.8	35.5	113.4	38	110.5	22.4
Gluteus medius	184.5	260	160.8	220.3	241	297.8
Gluteus minimus	43.9	60.4	85.3	120	98.8	131.6

All of the muscle loadings, except gluteus minimus, were distributed over muscle attachment areas to prevent excessive peak stresses. The gluteus minimus force was distributed uniformly over an area of 1 cm^2 around its resultant force location (P10 in Fig. 3). Table 2 shows the location of the resultant forces and the cross sectional area that the force was distributed over (the cross sectional area is represented by the square cross section length). This is illustrated in Fig. 3. The locations were taken from work by McMinn et al. (1984).

Table 2. Applied Loads coordinates based on McMinn et al. (1984) presented in Fig. 3

Joint Contact & Muscle Force	Location (cm)		Distribution length (cm)
	X	Y	
Hip Joint contact force	P1	10.37	2.15
	P2	9.52	
	P3	8.49	
Piriformis	P4	3.52	0.52
	P5	3.31	
	P6	3.08	
Gluteus medius	P7	2.84	1.07
	P8	2.31	
Gluteus minimus	P9	1.96	
	P10	1.41	

Using Eq. (2), and considering the maximum and minimum of the bone density as the limiting factors of the remodeling algorithm, the bone density in each time step Δt was updated as

$$\Delta\rho = (0.115 \times e^{-0.02t} + 0.05) \left(\sum_{i=1}^{2628} e^{-r_i/0.1} \left(\frac{U_i}{0.1125\rho_i} \right)^{1.5} - 1 \right) \Delta t \quad (5)$$

Here we assumed $\Delta t = 1.0$. The time step was chosen to guarantee that it was small enough, not to affect the end result in a significant way, and reduce iteration time.

In the first phase of simulation analysis the process starts with a uniform density distribution of $\rho_0 = 0.8 \text{ gr/cm}^3$. The Poisson's ratio was taken as 0.3 in all iterations. The following relation between module of elasticity and density was considered after Carter et al. (1977)

$$E = 3790\rho^3 \text{ and } \nu = 0.3 \quad (E \text{ is in "MPa" where } \rho \text{ is in "gr/cm}^3\text{"}) \quad (6)$$

The total mass (M) of the structure was calculated after every time step, from

$$M = \sum_{i=1}^n (V_i \rho_i) \quad (7)$$

where V_i and ρ_i are the volume and density of element i , and n is the number of elements in the structure. The convergence was assumed reached when the mass of the structure was stable. In most cases, convergence was achieved after about 200 iterations. It should be noted again that the objective of this remodeling rule was to achieve $U_a/\rho = k$ for every element in the structure. For those elements in which the algorithm indicated that the bone should be resorbed completely, the density was assigned a minimum number, ($\rho = \rho_{\min} = 0.01 \text{ gr/cm}^3$).

For the elements that the algorithm indicated the bone density should be greater than the cortical bone density, the maximum bone density was assigned, ($\rho = \rho_{\max} = 1.74 \text{ gr/cm}^3$).

RESULTS AND DISCUSSIONS

A typical converged density distribution with a set of parameters is shown in Fig. 4 ($\rho_0 = 0.8 \text{ gr/cm}^3$, $\alpha = 1.5$, $f_i(r) = e^{-r_i/R}$, $R = 0.1 \text{ cm}$).

The iterations continued until the mass of structure reached a constant. To understand the local mass redistributions which were not accounted for by considering the total mass in the convergence criteria, the change of density in each element after each iteration was evaluated. This approach ensures that the convergence is achieved both globally as well as locally. The results show that the bone density distribution obtained from the adaptive bone remodeling procedure is comparable with actual proximal femur bone density taken from DEXA data.

The effect of different influence functions on converged density pattern

Different remodeling algorithms may produce different density distribution patterns and convergence rates. A realistic density distribution comparable with the experimental data such as CT-scan or DEXA data with a high convergence rate may be affected by the choice of influence functions. In this research the effect of different coefficients and factors in the remodeling algorithm, (Eq. 2), on the bone density distribution was investigated.

As we discussed, “ R ” which is the influence range of the influence function $f_i(r)$ (Eq. 2) has a significant effect on the convergence. Here we considered eight different values for “ R ” ($R = 0.02, 0.04, 0.06, 0.08, 0.1, 0.2, 0.3$ and 0.4 cm) and investigated its effect on convergence rate and density distribution pattern. Furthermore, we studied the effect of using different influence functions, $f_i(r)$. A parabolic function instead of the exponential function was considered for this purpose. The parabolic functions considered in this investigation are shown in Fig. 9 and presented as;

$$\begin{cases} f_i(r) = -\left(\frac{r_i}{\tilde{R}}\right)^2 + 1 & \text{when } [r_i/\tilde{R}] < 1 \\ f_i(r) = 0 & \text{when } [r_i/\tilde{R}] > 1 \end{cases} \quad (8)$$

The effect of the influence parameter, \tilde{R} , on the bone density distribution and convergence rate was also investigated. \tilde{R} values considered in this investigation were 0.0001, 0.01, 0.1, 0.2, 0.3 and 1.0cm. The density distributions obtained by these two different functions (parabolic and exponential) were comparable with each other when their influence distances (R and \tilde{R}) are almost equal.

The converged density distribution pattern of proximal femur for different influence range parameters, R , in the influence function $f_i(r)$ and their mass convergence are shown in Fig. 10 and 11, respectively. The results indicate that there is not a significant difference between converged density distribution patterns for R values less than 0.3cm. However, the remodeling rule with the same time-step did not converge for $R > 0.3$. The same behavior was observed when using parabolic functions. The converged density distribution pattern of proximal femur for different influence parameter, \tilde{R} , in the parabolic influence function and their mass convergence are presented in Fig. 12 and 13 respectively. The divergence of remodeling algorithm occurred when \tilde{R} , was greater than 1 cm.

CONCLUSIONS

A two dimensional adaptive bone remodeling was developed to predict bone density of the proximal femur. The influence of different influence functions and parameters in the adaptive modeling on the converged bone density distribution and convergence rate was investigated. The results show that both influence functions (exponential and parabolic) and influence range do not have a significant effect on the converged density distribution. However, the influence range R and \tilde{R} should be chosen appropriately respect to element size for achieving convergence. It must be noted that R and \tilde{R} are the main factors controlling the impact on the neighboring element. Therefore, it is expected to have a significant effect on convergence.

Three important phases of the gait cycle, heel strike, mid stance, and push off, were employed as boundary conditions to the simulation. The bone density distribution of the proximal femur was obtained by averaging the bone density distributions obtained from these density distributions. The density distributions obtained by this procedure predicts a reasonably accurate density distribution, with an intramedullary canal and Ward's triangle in the femoral head.

REFERENCES

Bitsakos, C., Kerner, J., Fisher, I., Amis, A. A., 2005, "The effect of muscle loading on the simulation of bone remodeling in the proximal femur", *Journal of Biomechanics*, 38, pp. 133–139.

Cowin, S. C., Hegedus, D. H., 1976, "Bone remodeling I: theory of adaptive elasticity", *J. Elasticity*, 6, pp. 313-326.

Firoozbakhsh, K., Cowin, S. C., 1981, "An analytical model for Pauwels functional adaptation mechanism in bone", *J. Biomech. Eng.*, 103, pp. 247-252.

Galileo, G., 1638. *Discorsi e Dimostrazioni Matematiche in Torno a due Nuove Scienze Attenenti Alla Meccanica e i Movimenti Locali*. Elsevier, Leida.

Hart, R. T., Davy, D. T., Heiple, K. G., 1984, "A computational method of stress analysis adaptive elastic materials with a view toward application in strain induced remodeling", *J. Biomech. Eng.*, 106, pp. 342-350.

Hegedus, D. H., Cowin, S. C., 1976, "Bone remodeling II: small strain adaptive elasticity", *J. Elasticity*, 6, pp. 337-352.

Huiskes, R., Weinans, H., Grootenboer, H. J., 1992, "The behavior of adaptive bone-remodeling simulation models", *Journal of Biomechanics*, Vol. 25, No. 12, pp. 1425-1441.

Huiskes, R., Weinans, H., Grootenboer, H. J., Dalstra, M., Fundala, B., Slooff, T. J., 1987, "Adaptive bone-remodeling theory applied to prosthetic-design analysis", *Journal of Biomechanics*, 20, pp. 1135-1150.

Kerner, J., Huiskes, R., van Lenthe, G.H., Weinans, H., van Rietbergen, B., Engh, C.A., Amis, A.A., 1999, "Correlation between pre-operative periprosthetic bone density and post-operative bone loss in THA can be explained by strain-adaptive remodeling", *Journal of Biomechanics*, 32, pp. 695-703.

Mullender, M. G., Huiskes R., Weinans, H., 1994, "A physiological approach to the simulation of bone remodeling as a self-organizational control process", *Journal of Biomechanics*, Vol. 27, No. 11, pp. 1389-1394.

Roux, W., 1881, "Der Kampf der Theile im organismus", Engelmann, Leipzig.

Turner, A. W. L., Gillies, R. M., Sekel, R., Morris, P., Bruce, W., Walsh, W. R., 2005, "Computational bone remodeling simulations and comparisons with DEXA results", *Journal of Orthopaedic Research*, 23, pp. 705-712.

Weinans, H., Huiskes, R., Grootenboer, H., 1992, "Effects of material properties of femoral hip components on bone remodeling", *Journal of Orthopaedics Research*, 10 (6), pp. 845–853.

Weinans, H., Huiskes, R., Grootenboer, H., 1992, "The behavior of adaptive bone-remodeling simulation models", *Journal of Biomechanics*, Vol. 25, No. 12, pp/ 1425-1441.

Wolff, J.L., (original publication in 1892), "The law of bone remodeling" (translated by Marquet, P., Furlong, R.), Springer, Berlin.

Xinghua, Z., He, G., Dong, Z., Bingzhao, G., 2002, "A study of the effect of non-linearities in the equation of bone remodeling", *Journal of Biomechanics*, 35 (7), pp. 951–960.

Xinghua, Z., He, G., Bingzhao, G., 2005, "The application of topology optimization on the quantitative description of the external shape of bone structure", *Journal of Biomechanics*, 38, pp. 1612–1620.

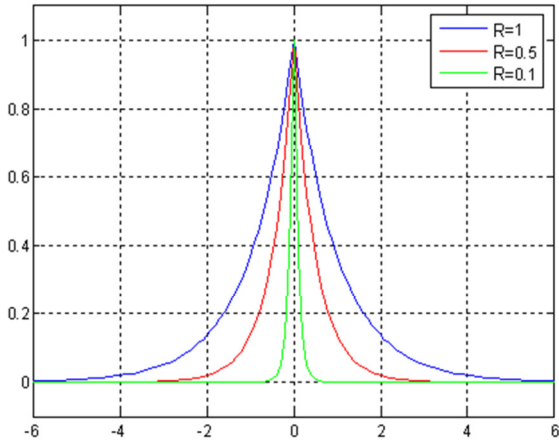


Fig. 1. The effect of spatial influence function “ $f_i(r)$ ” on adjacent elements for different influence distance “ R ”

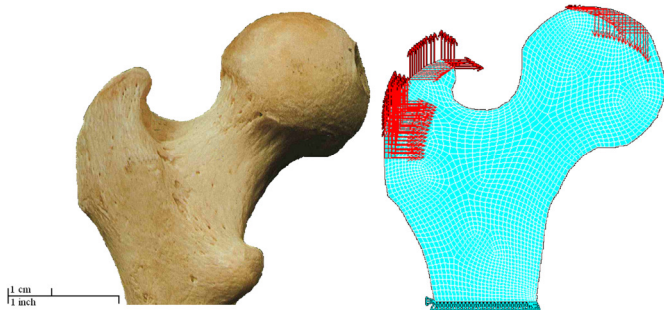


Fig. 2. Boundary condition and forces applied to the proximal Femur in the remodeling algorithm at 10% of the gait cycle

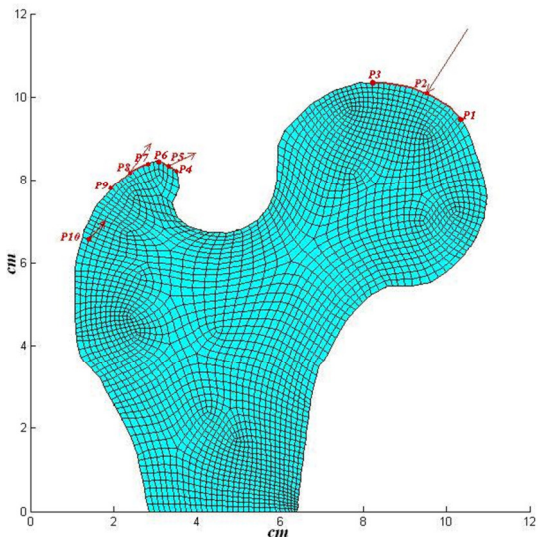


Fig. 3. Muscle loading and Hip joint contact force locations

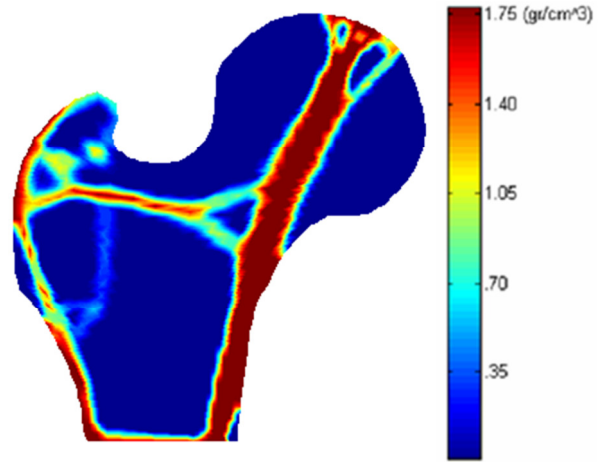


Fig. 4. Typical density distribution in proximal femur in the last iteration with selected parameters and function of ($\rho_0 = 0.8 \text{ gr/cm}^3$, $\alpha = 1.5$, $f_i(r) = e^{-r/R}$, $R = 0.1 \text{ cm}$).

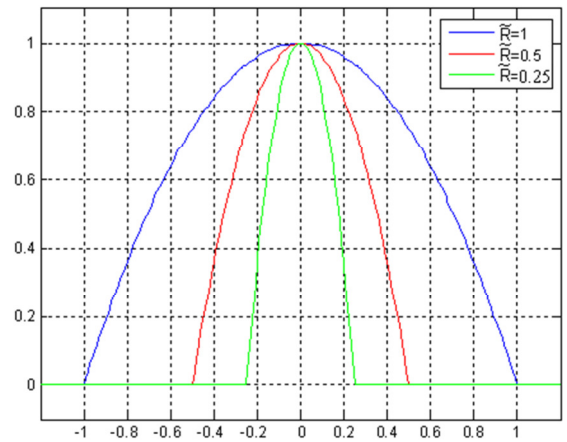


Fig. 5. The effect of parabolic influence function “ $f_i(r)$ ” on adjacent elements for different influence distance “ R ”

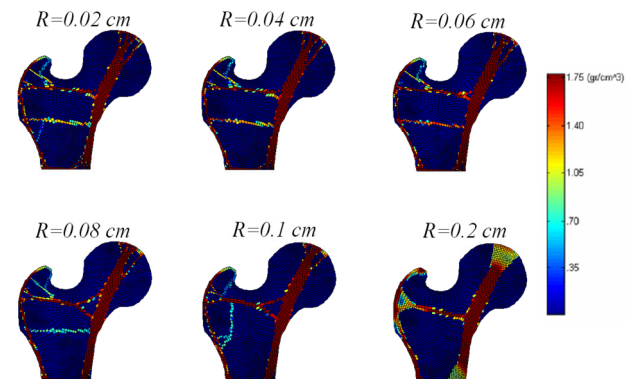


Fig. 6. The effect of influence distance “ R ” on the converged density distribution of proximal femur with ($\rho_0 = 0.8 \text{ gr/cm}^3$, $\alpha = 1.5$, $f_i(r) = e^{-r/R}$)

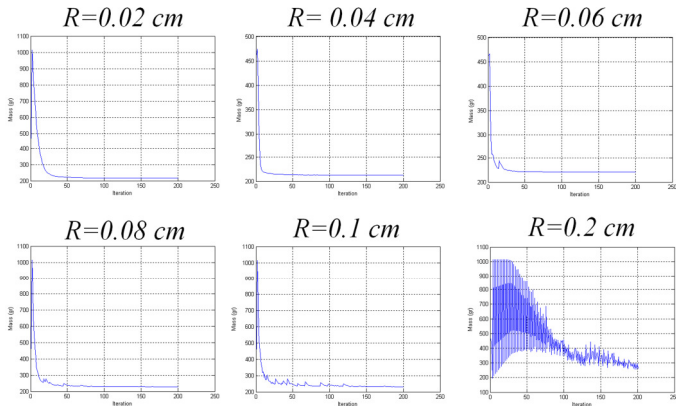


Fig. 7. The effect of influence distance “ R ” on the convergence of remodeling algorithm with $(\rho_0 = 0.8 \text{ gr/cm}^3, \alpha = 1.5, f_i(r) = e^{-r/R})$

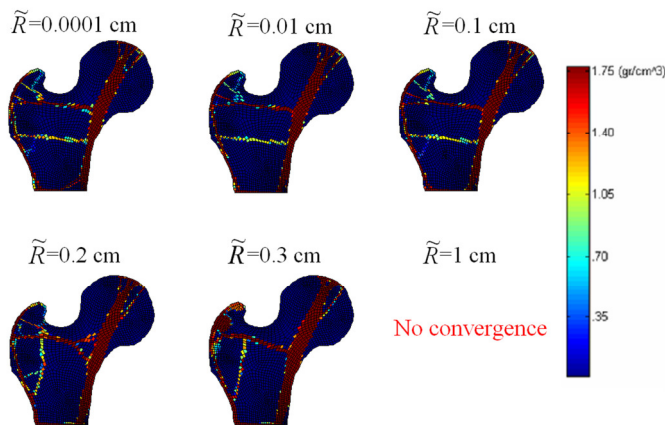


Fig. 12. The effect of influence distance “ \tilde{R} ” on the converged density distribution of proximal femur with $(\rho_0 = 0.8 \text{ gr/cm}^3, \alpha = 1.5, f_i(r) = -\left(\frac{r_i}{\tilde{R}}\right)^2 + 1)$

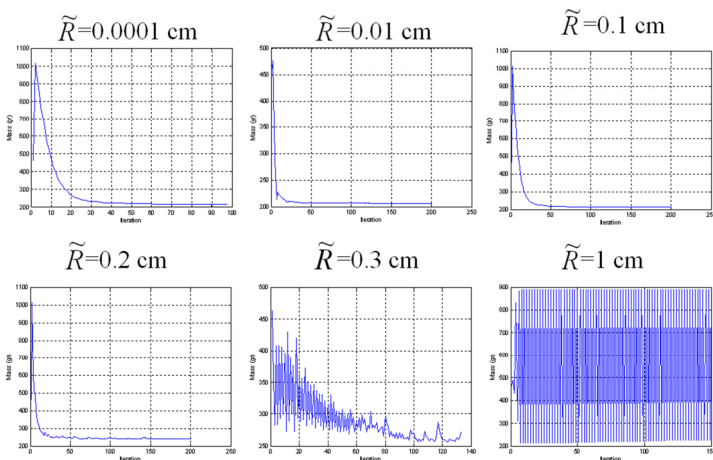


Fig. 13. The effect of influence distance “ \tilde{R} ” on the convergence of remodeling algorithm with $(\rho_0 = 0.8 \text{ gr/cm}^3, \alpha = 1.5, f_i(r) = -\left(\frac{r_i}{\tilde{R}}\right)^2 + 1)$

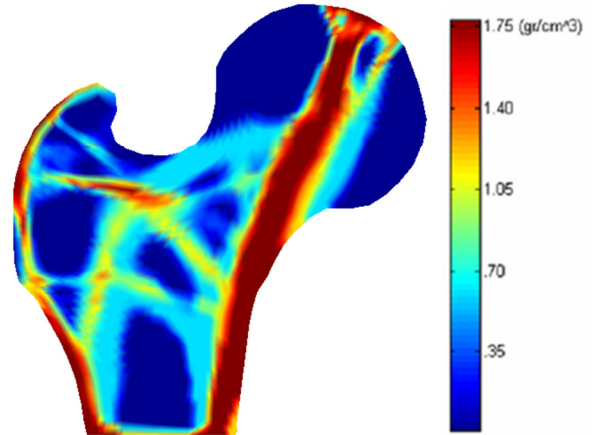


Fig. 15. Average density distribution of 10%

AUTHORS’ PROFILES:



Atiba J. Brereton, is currently pursuing his Master of Science (M.S.) in Mechanical Engineering. His areas of interest are Computer Aided Design (CAD) and Computer Aided Engineering (CAE).



Dr. Grant Warner is an Assistant Professor of Mechanical Engineering at Howard University. His research interests include bioengineering, energy harvesting, and design optimization.



Dr. Legand Burge is a Professor of Systems and Computer Science at Howard University. His interests include the application of distributed high performance computing.



Dr. Hamid Hashemi is a Professor of Mechanical Engineering at Northeastern University. Dr. Hashemi’s research interests are the design and analysis of composite and cellular materials.

Ali Marzban is a graduate student in the Department of Mechanical and Industrial Engineering at Northeastern University. His area of research is bone remodelling.